Materials Research Proceedings 44 (2024) 528-537 https://doi.org/10.21741/9781644903254-57

Optimizing deep drawing parameters for power battery shells through the integration of feature-weighted SVM and genetic algorithm

WANG Ruoda[1,a], SUN Yu[1,b*], WU Kai[1,c] and WANG Yu[1,d]

[1]Nanjing University of Science and Technology, Xiaolingwei No. 200 Street, 210094 Nanjing, China

[a]ruoda_wang@njust.edu.cn, [b]sunyu@njust.edu.cn, [c]wukai@njust.edu.cn, [d]wy@njust.edu.cn

Keywords: Deep Drawing, Finite Element Analysis, Feature-Weighted Support Vector Machine, Optimization, Power Battery Shells

Abstract. Deep drawing is one of the main forming processes for battery shells, and the rational setting of its process parameters directly affects the quality of the formation. Selecting the optimal deep drawing process parameters requires repeated trials and simulations, which increases the cost, reduces the efficiency, and poses a significant challenge to enterprises. To address this challenge, we focus on the first deep drawing process of the battery shell, proposing a parameter optimization method for battery shell deep drawing based on a Feature-Weighted Support Vector Machine (FWSVM) and Genetic Algorithms (GA). Our aim is twofold: on the one hand, to establish an agent model for finite element analysis of the deep drawing process using the FWSVM technique to enhance prediction accuracy and save simulation time; on the other hand, to derive optimal deep drawing process parameters using GA. The experimental results indicate that the FWSVM can accurately establish the relationship between process input/output parameters, and the optimized process parameters achieved through this method can realize the minimum thinning rate and convex mold contact force.

Introduction

The forming process of the rectangular power battery shell requires strict control over the process parameters, as the quality of forming directly affects the safety and stability of the battery [1]. Due to its unique geometric structure, the molding process for battery shells involves multiple deep drawings, stamping, and other complex processes [2]. Precise control of these processes is crucial for maintaining product consistency and quality. In the molding process, the battery shell's rounded corners undergo mainly tensile deformation, while its straight edges primarily experience bending deformation, due to varying forces [3]. The uneven forces and deformations complicate material flow, increasing the likelihood of defects like wrinkles and cracks. The first deep drawing stage is particularly prone to defects due to the substantial material deformation. Therefore, precise control of the process parameters at first deep drawing step becomes crucial to ensure the quality of the molding [4].

Modern numerical modeling and simulation techniques offer an efficient alternative to the costly and inefficient traditional trial-and-error methods. Simulating the molding process makes it possible to predict material behavior under specific parameters, enabling optimization of process parameters and mold design prior to production. This approach reduces trial-and-error iterations, cuts production costs, and accelerates product development [5].

Over the past few decades, researchers have focused on the optimization of deep drawing process. Park et al. [6] conducted finite element analysis on a multistage deep drawn punch featuring a high aspect ratio rectangle to focus on process design. Numerical methods were employed for analysis, which was then experimentally validated. To minimize material waste in the trimming process, simulations were performed in LS-DYNA3D using brick elements and explicit time integrals to optimize the billet shape. Yaghoubi et al. [7] investigated how die

geometry parameters affect the hydro-mechanical deep drawing process of 2024 aluminum alloy at high temperatures. Initially, they trained a neural network with the grouped data processing method (GMDH) to analyze process behavior, then optimized process variables using the Honeybee algorithm. The simulation results, validated against experimental data, demonstrated a strong correlation. Özek et al. [8] investigated the effects of die/blank holder angles, blank holder force, and die/punch diameters on the drawing limits, punch force, and wall thickness of DIN EN 10130–1999 steel sheets in angular squared deep drawing. Data was collected using profiles machined at angles ranging from 0° to 15° and 8, 12, and 16 mm diameters through a complete factorial design. Analysis techniques such as regression, signal-to-noise ratio, and ANOVA showed that increased angles and diameters extend drawing limits while reduced forces enhance surface uniformity. Padmanabhan et al. [9] explored optimizing die radius, blank holder force, and friction coefficient in deep drawing stainless steel cups via the finite element method and Taguchi technique. Findings indicate the die radius as the most critical parameter, followed by blank holder force and friction coefficient in terms of impact. Furthermore, adjusting the blank holder force and applying local lubrication significantly enhance the quality of formed parts, underscoring these parameters' key role in reducing manufacturing costs.

Despite extensive research on the deep drawing process by many scholars, there remains room for improvement. Firstly, in the design of the experiments method for agent model training, data is often assigned equal weights, neglecting the impact of feature weights on the model's performance. Secondly, relying on statistical analysis for optimization restricts process variable settings to a predetermined range of values. To address these issues, this study introduces an optimization method based on Feature-Weighted Support Vector Machine and Genetic Algorithms (FWSVM-GA) for the deep drawing process, specifically focusing on optimizing parameters in the battery shell's initial deep drawing process.

Methodology

The optimization framework of battery shell deep drawing process parameters by integrating FWSVM and GA:

The framework of FWSVM-GA method is shown in Fig. 1. Firstly, we designate the blank holder force (*BHF*), the punch fillet radius (R_p), the die fillet radius (R_d), the die gap (*DG*), and the friction conditions (*FC*) as input parameters. The thinning rate (*TR*) is chosen as an evaluation indicator and process output parameter. Subsequently, we use these input parameters as experimental factors, select four levels for each factor, and generate 111 experiments using the D-optimal experimental design method. Considering the different weights of input parameters, we determine the weight of each parameter through the entropy method. Then, these weights are applied to the classical support vector machine kernel function, resulting in the development of a FWSVM model. This model aims to establish a correlation between process parameters and output characteristics. Following this, we train and test the FWSVM model using input/output data from finite element analysis. We employ the FWSVM as a fitness function in a GA for optimizing process parameters. Lastly, the effectiveness of the finite element and agent models is verified through experiments.

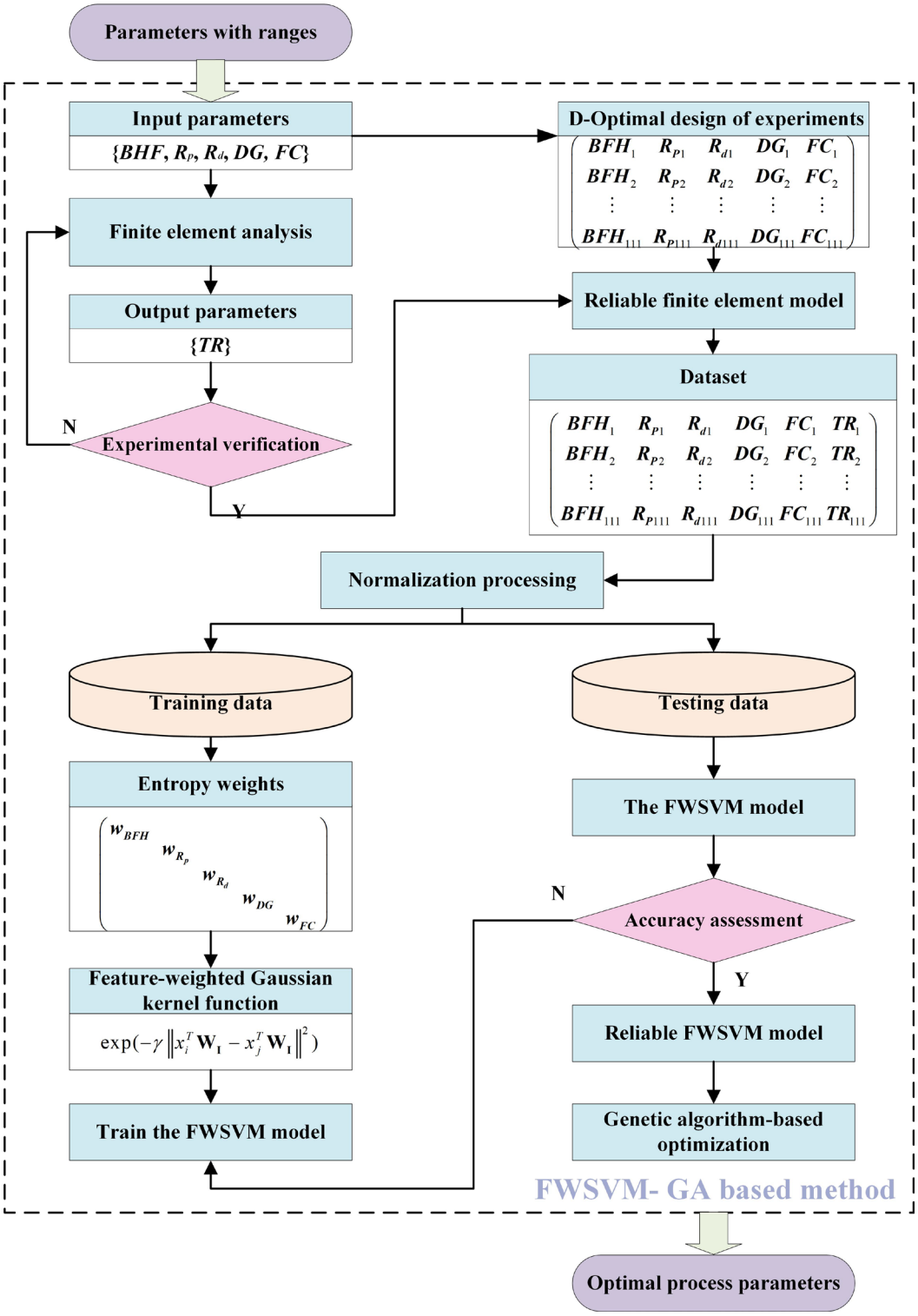

Fig. 1. The optimization framework of battery shell deep drawing process parameters by integrating FWSVM and GA.

Finite-element modeling. The power battery shell, characterized by its tall rectangular shape, requires multiple deep drawing processes for formation. This study primarily focuses on the initial deep drawing process of the battery shell. Fig. 2 shows the 3-D model after molding. The blank is made from a 1.5 mm thick rolled aluminum alloy sheet (AL3003H14), featuring a density of 2.7×103 kg/m^3, an elasticity modulus of 69 GPa, a yield strength of 125 MPa, and a tensile strength of 150 MPa.

Based on experience, the die's cross-section is elliptical, with a long semi-axis of 120.85 mm and a short semi-axis of 83.84 mm. The punch, die, part, and blank holder's 3-D models were initially crafted in SolidWorks and then converted to IGS format. For simulation, the part is initially imported into DYNAFORM software. Using the one-shot expansion method generates the blank shape, followed by the sequential import of the remaining models. In the meshing process, the punch, die, and blank holder are considered rigid bodies, with a cell size of 3mm and a thickness of 5 layers. The finite element model is depicted in Fig. 3. The initial deep drawing height is 80 mm, with a virtual drawing speed of 2 m/s. Parameters are configured and submitted to LS-DYNA for analysis, with post-processing conducted using eta/POST.

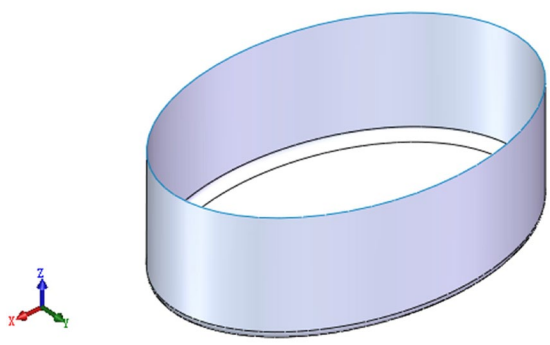

Fig. 2. 3-D model after drawing.

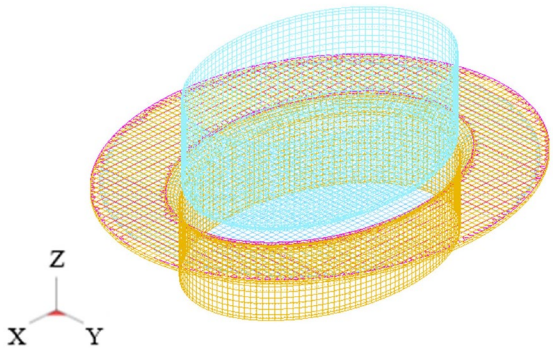

Fig. 3. Finite element model.

Orthogonal experimental design. One of the main objectives of this study is to predict the product quality under different process parameters. Finite element modeling, while useful for this purpose, is time-intensive due to the lengthy duration of each FE model run. Consequently, FWSVM is utilized as a more efficient technique to estimate process responses for specific sets of process parameters. Required data was collected through a series of simulation runs using the design of experiments (DOE) methodology.

Several process parameters, such as blank holder force, punch fillet radius, die fillet radius, die clearance, friction conditions, and blank size, jointly influence the quality of the battery shell's first deep drawing. Blank size has a minimal impact on forming. Using a larger blank optimizes material use, while a smaller blank can result in insufficient trimming allowance, impacting accuracy. Blank dimensions are derived from the part shape in DYNAFORM in this study. the blank holder force (*BHF*), the punch fillet radius (R_p), the die fillet radius (R_d), the die gap (*DG*), and the friction conditions (*FC*) as inputs, with each factor having four levels, as detailed in Table 1. For a complete factorial design, the number of possible designs is $N=L^m$, where L is the number of levels for each factor and m is the number of factors. Consequently, the full factorial design in this study encompasses 576 experiments. To further reduce simulation runs, a D-optimal experiment design was implemented. As a result, only 111 runs are necessary to gather the data needed for the FWSVM. The dataset was generated by obtaining the maximum thinning rate (*TR*) from all 111 experiments via FEA. In engineering applications, the thinning rate should not exceed 25%; Table 2 presents some of the datasets.

Table 1. Variable parameters with their levels.

Levels	*BHF* (mm)	R_p (mm)	R_d (mm)	*DG* (mm)	*FC*
1	30	10	11	1.65	0.13
2	40	11	12	1.8	0.15
3	50	12	13	1.95	0.17
4	60	13	14	2.1	0.19

Table 2. Dataset.

Levels	*BHF* (mm)	R_p (mm)	R_d (mm)	*DG* (mm)	*FC*	*TR*
1	50	10	11	2.1	0.13	19.268
2	40	11	13	2.1	0.13	12.242
3	60	12	12	1.8	0.19	14.798
⋮	⋮	⋮	⋮	⋮	⋮	⋮
110	60	11	11	1.95	0.17	17.941
111	30	11	14	1.8	0.13	14.574

The proposed FWSVM. Since different input parameters have different effects on the results during drawing, we propose to use weighted support vector machines for modeling. Let $D_{\text{train}} = (x_i, y_i)$ be the training dataset, where $x_i \in R^n$ is the i-th input feature, $y_i \in \{-1, +1\}$, $i = 1, 2, \ldots, l$, is the class label. Suppose the hyperplane correctly divides the D_{train} into two classes, in that case, the optimal hyperplane should maximize the sum of the minimum distances from the two classes of samples to the hyperplane.

The optimal hyperplane is obtained by solving the following optimization problem:

$$\begin{aligned} &\min_{\omega,b,\xi_i} : \frac{1}{2}\|\omega\| + C\sum_{i=1}^{n}\xi_i \\ &\text{suject to:} \begin{cases} y_i[\omega\cdot\phi(x\mathrm{W})+b] \geq 1-\xi,\ i=1,2,\cdots,n \\ \xi_i \geq 0,\ i=1,2,\cdots,n \end{cases} \end{aligned} \tag{1}$$

where C is a positive constant parameter used to control the tradeoff between the margin and the classification error. ξ_i denotes slack variables, ϕ is the feature mapping function, which maps the input space to a usually high dimensional feature space where the data points become linearly separable, $\mathrm{W}_{n\times n}$ represents a feature weighted matrix.

Since Eq. 1 is a convex quadratic programming problem, using the Lagrange multiplier method, its Lagrange function is shown as follows,

$$L(\omega,b,\alpha,\xi,\mu) = \frac{1}{2}\|\omega\| + C\sum_{i=1}^{n}\xi_i + \sum_{i=1}^{n}\alpha_i[1-\xi_i - y_i(\omega\cdot\phi(x_i\mathrm{W})+b)] - \sum_{i=1}^{n}\mu_i\xi_i \tag{2}$$

where α_i and μ_i are Lagrange multipliers. Letting the partial derivatives of $L(\omega, b, \alpha, \xi, \mu)$ with respect to ω, b, ξ_i be 0 yields：

$$\omega = \sum_{i=1}^{n}\alpha_i y_i x_i \tag{3}$$

$$0 = \sum_{i=1}^{n}\alpha_i y_i \tag{4}$$

$$C = \alpha_i + \mu_i \tag{5}$$

Bringing Eq. 3-5 into Eq. 2 to get the dual problem of Eq. 1,

$$\begin{aligned} &\max_{\alpha} : \sum_{i=1}^{n} \alpha_i - \frac{1}{2} \sum_{i=1}^{n} \sum_{j=1}^{n} \alpha_i \alpha_j y_i y_j \phi(x_i \mathrm{W}) \phi(x_j \mathrm{W}) \\ &\text{subject to: } \sum_{i=1}^{n} \alpha_i y_i = 0 \\ &\qquad 0 \le \alpha_i \le C \end{aligned} \tag{6}$$

For the solution of Eq. 6, the Karush–Kuhn–Tucker (KKT) conditions [10] require:

$$\begin{cases} \alpha_i \ge 0,\ \mu_i \ge 0, \\ y_i(\omega \cdot \phi(x_i \mathrm{W}) + b) - 1 + \xi_i \ge 0, \\ \alpha_i [y_i(\omega \cdot \phi(x_i \mathrm{W}) + b) - 1 + \xi_i] = 0, \\ \xi_i \ge 0,\ \mu_i \xi_i = 0. \end{cases} \tag{7}$$

Then *b* can be calculated as:

$$b = y_j - \omega \cdot \phi(x_j \mathrm{W}) \tag{8}$$

Since the value of b is not unique, its average value is taken,

$$\bar{b} = \frac{1}{N} \sum_{0 \le \alpha_j \le C} [y_j - \sum_{i=1}^{n} \alpha_i y_i (\phi(x_i \mathrm{W}) \phi(x_j \mathrm{W}))] \tag{9}$$

where N is the number of support vectors. Then the corresponding decision function is denoted as,

$$f(x) = sign(\omega \cdot \phi(x \mathrm{W}) + \bar{b}) \tag{10}$$

In order to express FWSVM, The feature weighted kernel function $K_f(x_i, x_j)$ is defined as follows:

$$K_f(x_i, x_j) = \phi(x_i \mathrm{W}) \cdot \phi(x_j \mathrm{W}) = K_p(x_i \mathrm{W}, x_j \mathrm{W}) \tag{11}$$

Only the individual features were weighted in this study, so W is a diagonal matrix of order *n*. At this point $(\mathrm{W})_{ii} = e_i$ ($1 \leqslant i \leqslant n$) represents the weight of the *i*-th feature, and in general e_i is not all equal.

$$\mathrm{W} = \begin{pmatrix} e_1 & & & \\ & e_2 & & \\ & & \ddots & \\ & & & e_n \end{pmatrix} \tag{12}$$

Therefore, the non-linear classification decision function is,

$$f(x) = sign(\sum_{i=1}^{n} \alpha_i y K_f(x_i, x_j) + \frac{1}{N} \sum_{0 \le \alpha_j \le C} [y_j - \sum_{i=1}^{n} \alpha_i y_i K_f(x_i, x_j)]) \tag{13}$$

the Feature-weighted Gaussian radial basis function is adopted as kernel function,

$$K_f(x_i, x_j) = [\gamma(x_i \mathrm{W}) \cdot (x_j \mathrm{W}) + r]^d = (\gamma x_i \mathrm{W}\mathrm{W}^T x_j^T + r)^d,\ \gamma > 0 \tag{14}$$

This study uses the entropy weight method to determine the weight of each input parameter, which is an objective assignment method commonly used in multi-indicator comprehensive evaluation problems. It reflects the dispersion of the indicators by calculating the entropy value of each indicator, and then determines the weight of each indicator. The smaller the entropy value, the greater the variability of the indicator, the more information it carries, so it should be given a larger weight.

Firstly, we construct the input parameters into a matrix V,

$$\mathrm{V} = \begin{pmatrix} p_{11} & p_{11} & \cdots & p_{1m} \\ p_{21} & p_{22} & \cdots & p_{2m} \\ \vdots & \vdots & \ddots & \vdots \\ p_{k1} & p_{k2} & \cdots & p_{km} \end{pmatrix} \tag{15}$$

where p_{ij} represents the value of the j-th index in the i-th case (i = 1, 2, 3, …, k, j = 1, 2, 3, …, m).

Using Eq. 16 to normalize the elements in matrix V to obtain the matrix Q = $(q_{ij})_{k\times m}$.

$$q_{ij} = \frac{p_{ij}}{\sum_{i=1}^{m} p_{ij}} \tag{16}$$

The entropy weight is obtained via:

$$\begin{aligned} e_{\mathrm{o}j} &= -\frac{1}{\ln m}\sum_{j=1}^{m} q_{ij} \ln q_{ij} \\ g_j &= 1 - e_{\mathrm{o}j} \\ w_{\mathrm{o}j} &= \frac{g_j}{\sum_{j=1}^{m} g_j} \end{aligned} \tag{17}$$

where $e_{\mathrm{o}j}$ represents the entropy value of index j, g_j is the variation coefficient, the smaller the value of $e_{\mathrm{o}j}$, the larger the value of g_j, and the greater the contribution of the attribute, $w_{\mathrm{o}j}$ denotes the weight. The objective weight vector W can be written as,

$$\mathrm{W} = \left(w_{\mathrm{o}1},\ w_{\mathrm{o}2},\ ...,\ w_{\mathrm{o}j},\ ...,\ w_{\mathrm{o}m}\right) \tag{18}$$

To validate the superiority of FWSVM, we compare it with other commonly used agent models (SVM, BPNN). We use leave-one-out cross-validation (LOO-CV) to estimate the performance of comparative methods and employ the mean absolute percentage error (MAPE) to measure the discrepancy between computed and FEM values. The accuracy for each LOO-CV iteration can be calculated as follows:

$$\mathrm{acc} = 1 - MAPE = 1 - \frac{1}{n}\sum_{i=1}^{N}\left|\frac{TR_i - y_i}{TR_i}\right| \tag{19}$$

where n is the number of samples, TRi is the finite element simulation value and yi is the predicted value.

Optimization of deep drawing process parameters. The objective of this section is to identify optimal process parameters through Genetic Algorithms (GA). Drawing on Darwin's principles of natural selection and genetics, GA is a search algorithm that emulates the natural evolutionary process to tackle optimization and search challenges.GA is capable of conducting a global search across the search space, addressing complex issues with numerous objectives and constraints to identify the global optimal solution or one nearing the global optimum.

In this study, FWSVM serves as the GA's fitness function, aiming to identify optimal deep drawing parameter values. During the optimization search, outputs below 25% receive a fitness value that increases inversely with the output value. Concurrently, a substantial negative penalty is applied for unsatisfactory solutions to steer the algorithm away from these options. For predicted outputs under 25%, a fitness value is assigned using the formula - (25 - output). This approach aims to increase fitness (in absolute terms) as output diminishes, maintaining a negative fitness to identify parameter combinations yielding the smallest possible FWSVM model outputs under 25%. The input parameters were constrained to BHF (kN): [30, 60], Rp (mm): [10, 13], Rd (mm): [11, 14], DG (mm): [1.65, 2.1], FC: [0.13, 0.19]. After 50 iterations, the algorithm concludes, with optimal parameters for each iteration displayed in Fig. 4. Final optimal parameter combinations is detailed in Table 3.

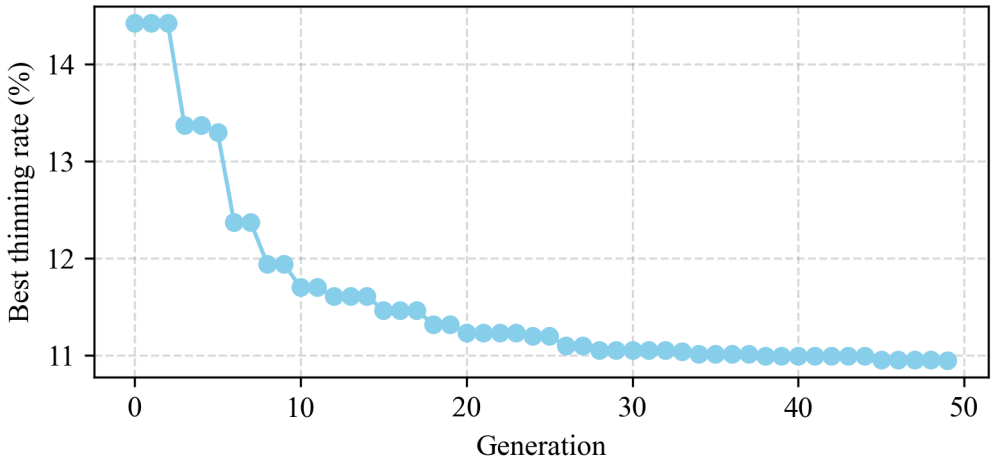

Fig. 4. Iteration process.

Table 3. Optimal parameter combination.

BHF (mm)	R_p (mm)	R_d (mm)	*DG* (mm)	*FC*	*TR (%)*
52.153	13.012	13.995	2.037	0.171	10.945

Result and discussion

As shown in Fig. 5, the weights of the five input parameters were calculated using Eq. 15-18. These weights were used to construct the FWSVM. Using Eq. 19, we computed the accuracy of the FWSVM with respect to the SVM, and the BPNN (default values were used for the parameters of the SVM and the BPNN), and the results are shown in Fig. 6.

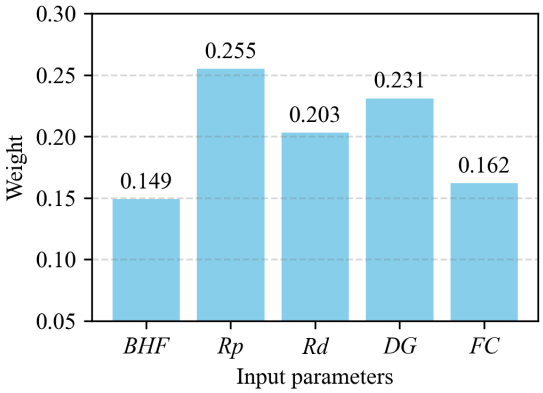

Fig. 5. Weighting distribution.

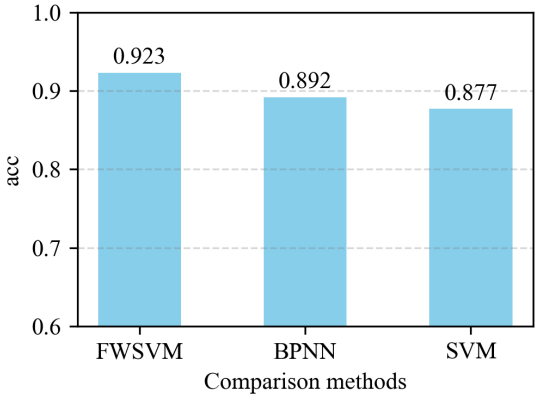

Fig. 6. Accuracy comparison.

According to Fig. 5, in constructing the FWSVM for enhanced prediction accuracy, R_p holds the highest weight, while *BHF* has the lowest, with the overall weight ranking as $R_p > DG > R_d > FC > BHF$. However, this ranking is based on the dataset's dispersion and does not reflect the parameters' significance for deep drawing molding quality. From Fig. 6, it can be seen that all three methods achieve good prediction results, Specifically, FWSVM leads in accuracy at 0.923, followed by BPNN at 0.892, with SVM trailing at 0.877. These results demonstrate FWSVM's superiority.

We also performed finite element analysis and experimental verification on the optimal process parameter combinations in Table 3. The results of the finite element analysis are shown in Fig. 7, and the experimental parts are shown in Fig. 8.

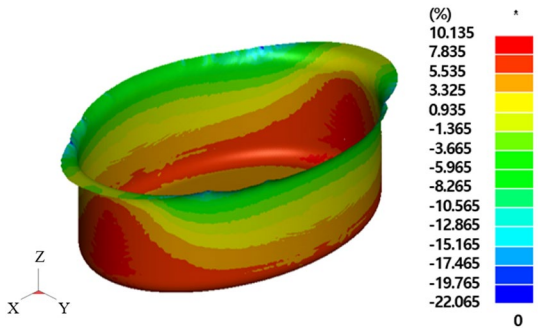

Fig. 7. The finite element analysis results.

Fig. 8. The experimental result.

From Fig. 7, it can be seen that the maximum thinning rate of the part under the optimal parameter combination is 10.135%, which is much less than the limiting value of 25%. The difference between the finite element simulation results and the predicted results (10.945%) is only 0.81%, which further illustrates the accuracy of FWSVM. The experimental results Fig. 8 show that the parts are free from defects such as rupture and wrinkle and possess excellent quality.

Summary

This study employs the FWSVM technique to develop an agent model for finite element analysis of the deep drawing process, enhancing prediction accuracy and reducing simulation time. Subsequently, GA is applied to identify the deep drawing process's optimal parameters, thereby elevating the molding quality of the battery shell's initial deep drawing. As input parameters, we selected blank holder force (*BHF*), punch fillet radius (R_p), die fillet radius (R_d), die gap (*DG*), and friction conditions (*FC*). Thinning rate (*TR*) is chosen as the output parameter. The FWSVM

dataset is generated through the design of experiments method and finite element analysis. The trained FWSVM serves as the fitness function for GA, leading to the identification of the optimal process parameter combination. Experimental evidence shows that battery shells' initial deep drawn parts exhibit outstanding quality under this set of process parameters.

References

[1] T.D. Nguyen, J. Deng, B. Robert, W. Chen, T. Siegmund, Deformation Behavior of Single Prismatic Battery Cell Cases and Cell Assemblies Loaded by Internal Pressure, J. Electrochem. Energy Conversion Storage 18 (2021). https://doi.org/10.1115/1.4050101

[2] Q. Yu, Y. Nie, S. Peng, Y. Miao, C. Zhai, R. Zhang, J. Han, S. Zhao, M. Pecht, Evaluation of the safety standards system of power batteries for electric vehicles in China, Appl. Energy 349 (2023) 121674. https://doi.org/10.1016/j.apenergy.2023.121674

[3] S. Yaghoubi, F. Fereshteh-Saniee, An investigation on the effects of the process parameters of hydro-mechanical deep drawing on manufacturing high-quality bimetallic spherical-conical cups, Int. J. Adv. Manuf. Technol. 110 (2020) 1805–1818. https://doi.org/10.1007/s00170-020-05985-5

[4] R. Dwivedi, G. Agnihotri, Study of Deep Drawing Process Parameters, Materials Today: Proceedings 4 (2017) 820–826. https://doi.org/10.1016/j.matpr.2017.01.091

[5] M. Manoochehri, F. Kolahan, Integration of artificial neural network and simulated annealing algorithm to optimize deep drawing process, Int. J. Adv. Manuf. Technol. 73 (2014) 241–249. https://doi.org/10.1007/s00170-014-5788-5

[6] C.S. Park, T.W. Ku, B.S. Kang, S.M. Hwang, Process design and blank modification in the multistage rectangular deep drawing of an extreme aspect ratio, J. Mater. Process. Technol. 153–154 (2004) 778–784. https://doi.org/10.1016/j.jmatprotec.2004.04.306

[7] S. Yaghoubi, F. Fereshteh-Saniee, Optimization of the geometrical parameters for elevated temperature hydro-mechanical deep drawing process of 2024 aluminum alloy, Proceedings of the Institution of Mechanical Engineers, Part E: J. Process. Mech. Eng. 235 (2021) 151–161. https://doi.org/10.1177/0954408920949364

[8] C. Özek, E. Ünal, Optimization and Modeling of Angular Deep Drawing Process for Square Cups, Mater. Manuf. Process. 26 (2011) 1117–1125. https://doi.org/10.1080/10426914.2010.532526

[9] R. Padmanabhan, M.C. Oliveira, J.L. Alves, L.F. Menezes, Influence of process parameters on the deep drawing of stainless steel, Finite Elements in Analysis and Design 43 (2007) 1062–1067. https://doi.org/10.1016/j.finel.2007.06.011

[10] S.P. Boyd, L. Vandenberghe, Convex optimization, Cambridge University Press, Cambridge, UK ; New York, 2004